

Box diagram in the elastic electron-proton scattering

Dmitry Borisyuk and Alexander Kobushkin*

*Bogolyubov Institute for Theoretical Physics
Metrologicheskaya str. 14-B, 03143, Kiev, Ukraine*

(Dated: January 25, 2020)

We present exact evaluation of box diagram for the elastic ep scattering with proton in the intermediate state. Using analytic properties of the proton form factors, we express the amplitude via twofold integral, which involves the form factors in the space-like region only. Therefore experimentally measured form factors can be used in the calculations directly. The numerical calculation is done with the form factors extracted by Rosenbluth as well as by polarization transfer methods. The dependence of the results on the form factor choice is small for $Q^2 \lesssim 6 \text{ GeV}^2$, but becomes sizable at higher Q^2 .

I. INTRODUCTION

Study of the elastic electron-proton scattering

$$e^- + p \rightarrow e^- + p \quad (1)$$

is an important source of information about the proton structure. In the first order of the perturbation theory (PT) or Born approximation the reaction amplitude

$$\mathcal{M}_{\text{Born}} = \frac{4\pi\alpha}{q^2} \bar{u}' \gamma_\mu u \cdot \bar{U}' \Gamma^\mu(q) U \quad (2)$$

is expressed in terms of Dirac and Pauli proton form factors (FFs), F_1 and F_2 ,

$$\Gamma_\mu(q) = F_1(q^2) \gamma_\mu - F_2(q^2) [\gamma_\mu, \gamma_\nu] \frac{q^\nu}{4M}, \quad (3)$$

where u , U , u' , U' are 4-spinors of incoming and outgoing particles, $\alpha \approx 1/137$ is fine structure constant, q is the momentum transfer from the electron to the proton. The linear combinations, $G_E = F_1 - \frac{q^2}{4M^2} F_2$ and $G_M = F_1 + F_2$, called the electric and magnetic FFs, are also widely used.

During many years it was a common practice to extract FFs by the Rosenbluth separation method. FFs obtained by this method obey with good accuracy $G_E/G_M = \text{const}$ for $0 < Q^2 \lesssim 6 \text{ GeV}^2$ ($Q^2 \equiv -q^2$). However since 2000 series of experiments was done using an alternative, polarization transfer method [1]. These experiments yielded strikingly different results: G_E/G_M ratio decreased linearly with Q^2 . Since both methods are based on the Born approximation, the reason for discrepancy is likely the neglected higher order PT terms. There are two types of second order Feynman diagrams: first, diagrams, involving an exchange of only one virtual photon (vacuum polarization or vertex corrections) and second, two photon exchange or box diagram, Fig.1(a). The part of amplitude, coming from one-photon exchange diagrams, has the structure similar to (2) (certainly with another functions in place of $F_{1,2}$) and cannot lead to the discrepancy between two methods. Such diagrams are usually taken into account in experimental analyses.

Therefore the two photon exchange diagram plays the key role in understanding the experimental results and extracting correct FF values.

The lower part of the diagram represents the doubly virtual Compton scattering (VVCS) off the proton. The amplitude of VVCS has two poles which are due to single proton in the intermediate state. The contribution of these poles to the box diagram is called the elastic contribution. Similar contributions appear from $\Delta(1232)$ and other resonances, Fig.1. In the present paper we study the elastic contribution only (diagrams Fig.1(b) and (c), which we later on call box (in the narrow sense) and x-box diagrams). We also believe that the method derived here can be applied, with minor modifications, to the contributions of resonances. This will be the subject of a separate paper.

In previously published papers the box diagram was calculated in several, more or less approximate ways.

*Electronic address: kobushkin@bitp.kiev.ua

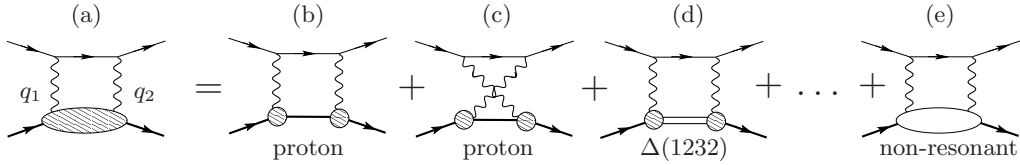


FIG. 1: Two photon exchange for the elastic ep scattering.

First is the soft photon approximation used in Tsai's paper [2] (and also in Ref.[3]). It is assumed that the main contribution to the loop integral comes from the $q_1 \approx 0$, $q_2 \approx q$ and $q_1 \approx q$, $q_2 \approx 0$ regions. The reason is usually given that the integrand is strongly peaked at that points because of the infrared (IR) singularity. However, only the IR divergent part (which exactly cancels in the final answer), can be calculated in such a way. Instead, we are interested here in the IR finite part, and it is by no means obvious, that the main contribution to it comes from the same regions.

The second way, which may be called "hard photon approximation", assumes the most important region to be $q_1 \approx q_2 \approx q/2$ [4]. This may be a reasonable assumption, however we believe it needs justification. In Ref.[4], after making the approximation the loop integral becomes divergent and fairly arbitrary ultraviolet cut-off is used, introducing the additional uncertainty of the result.

In the third group of papers the loop integral was calculated exactly, however using the special FF parameterization, monopole FF in Ref.[5] and the sum of monopoles in Ref.[6],

$$F_{1,2}(t) = \sum_i \frac{n_i}{d_i - t}, \quad (4)$$

where n_i and d_i are fitted constants. Thanks to this simple form, the resulting integrals are expressed through 4- and 3-point functions, which were calculated numerically using computer program.

However, such sort of calculation has the following problem. Since the FFs, entering the integral, are not known from the first principles, we should use some model for them or fit to experiment ¹. The problem is that only $t < 0$ region is accessible for the scattering experiments. While the $t > 4M^2$ region can, in principle, be studied in $e^- + e^+ \rightarrow p + \bar{p}$ reaction, the unphysical region $0 < t < 4M^2$ is completely inaccessible. But the loop integral involves FFs in the time-like region ($t > 0$) as well. A natural question arises, how the (largely unknown) FF behaviour for $t > 0$ influences the total result. In particular, parameterization used in Ref.[6] does not even roughly reproduce FFs in the $t > 0$ region. Indeed, unitarity requires that FFs have poles at $t = m_V^2$ where m_V are masses of vector mesons, namely ρ -, ω - and φ - mesons (neglecting their widths). But the numerical values given in Ref.[6] are away from these masses. So, the fit is not suitable for $t > 0$ and the results of Ref.[6] cannot be considered reliable before answering the above question.

In the present paper we calculate the box and x-box diagrams in the most rigorous way. First, contrary to [2, 3, 4] we evaluate all integrals exactly, without any restriction of the integration domain. Second, contrary to [5, 6] we do not use any special assumptions on the FFs functional form. We perform the analytical integration to the maximal possible extent, resulting in

$$\mathcal{M}_{\substack{\text{box} \\ \text{x-box}}} = \sum_{i,j=1}^2 \int_{t_1, t_2 \leq 0} \mathcal{K}_{ij}(t_1, t_2) F_i(t_1) F_j(t_2) dt_1 dt_2, \quad (5)$$

where $\mathcal{K}_{ij}(t_1, t_2)$ is explicitly known. We found, that thanks to FF analyticity the integration in (5) is done over negative t_1 and t_2 only. Therefore we overcome the above-mentioned problem of finding out FF values at $t > 0$. Now the experimentally measured FFs can be used directly for the calculation of (5). In particular, now we are able to calculate the box diagram with the FFs as extracted by polarization transfer measurements, which was impossible in the approach of Refs.[5, 6].

Then we calculate two photon exchange amplitudes numerically using different FF parameterizations and discuss the results.

¹ Of course, this is a vicious circle, since the accurate FF extraction from experiment implies taking into account the box diagram. However as a zeroth approximation we may neglect it; then some iterative procedure may be used to obtain precise result.

II. THE METHOD

The box and x-box diagrams, as well as notation for particle momenta, are displayed in Fig.2. Thin line is for electron, thick is for proton. The proton and electron masses are M and m , respectively. We also denote

$$P = (p + p')/2, \quad K = (k + k')/2, \quad q = p' - p. \quad (6)$$

The following relations are fulfilled:

$$q_1 = p'' - p, \quad q_2 = p'' - p', \quad k'' = K \pm (P - p''), \quad (7)$$

upper sign is for the box, lower is for the x-box diagram.

The amplitude corresponding to either of diagrams is

$$i\mathcal{M}_{\text{box}} = \left(\frac{\alpha}{\pi}\right)^2 \int \frac{N(p'')d^4p''}{(q_1^2 - \lambda^2)(q_2^2 - \lambda^2)(k''^2 - m^2)(p''^2 - M^2)}, \quad (8)$$

where

$$N(p'') = \bar{u}' \gamma_\mu (\hat{k}'' + m) \gamma_\nu u \cdot \bar{U}' \Gamma_\mu(q_1) (\hat{p}'' + M) \Gamma_\nu(q_2) U, \quad (9)$$

Γ_μ is defined by (3). For the x-box diagram one should interchange γ_μ with γ_ν . The “photon mass” λ is introduced in the denominator to avoid IR divergence. Though the electron mass is small compared to the characteristic energies involved, we will not neglect it in the denominator, first, for generality, second, since, as it is seen from the result, each of the diagrams diverges like $\ln m$ as $m \rightarrow 0$ (but their sum does not).

In general case the elastic ep scattering is described by six invariant amplitudes. However three of them are proportional to m , so in the $m \rightarrow 0$ limit remain only three [7]:

$$\mathcal{M} = \frac{4\pi\alpha}{q^2} \bar{u}' \gamma_\mu u \cdot \bar{U}' \left(\tilde{F}_1 \gamma^\mu - \tilde{F}_2 [\gamma^\mu, \gamma^\nu] \frac{q_\nu}{4M} + \tilde{F}_3 \hat{K} \frac{P^\mu}{M^2} \right) U. \quad (10)$$

The invariant amplitudes \tilde{F}_i depend on two kinematic variables, $\nu = 4PK$ and $t = q^2$. In the first order of PT $\tilde{F}_1(\nu, t) = F_1(t)$, $\tilde{F}_2(\nu, t) = F_2(t)$, $\tilde{F}_3(\nu, t) = 0$. The contribution of the box diagram to any of these amplitudes is given by the integral, similar to (8), but with another numerator,

$$N(p'') = \sum_{i,j=1}^2 A_{ij}(p'') F_i(q_1^2) F_j(q_2^2), \quad (11)$$

where $A_{ij}(p'')$ are some (rather cumbersome) explicitly known scalar polynomial functions of p'' . To simplify the notation, from now on we drop the sum sign and the summation indices in the expressions like (11) and write them simply as $A(p'') F(q_1^2) F(q_2^2)$. However the summation is always understood.

There are at most four independent scalar functions of p'' , say, p''^2 , pp'' , $p'p''$ and Kp'' (the pseudoscalar combination $\epsilon_{\mu\nu\sigma\tau} p''^\mu p^\nu p'^\sigma K^\tau$ cannot appear because of the parity considerations). The alternative, more convenient choice is

$$\begin{aligned} p''^2 - M^2, \\ k''^2 - m^2 = \frac{t_1 + t_2 - t}{2} \pm 2KP \mp 2Kp'', \\ t_1 \equiv q_1^2 = p''^2 + M^2 - 2pp'', \\ t_2 \equiv q_2^2 = p''^2 + M^2 - 2p'p'', \end{aligned} \quad (12)$$

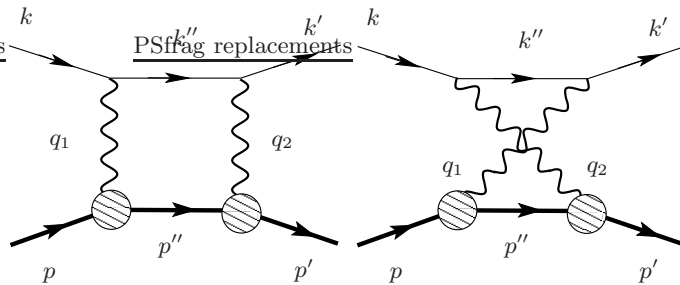


FIG. 2: Box diagram (left) and x-box diagram (right) with the proton in the intermediate state.

upper sign is for the box, lower is for the x-box diagram. Since $A_{ij}(p'')$ are polynomials in p'' , they can also be written as polynomials in four variables (12).

Now it is easy to see that the integral (8) can be reduced to the four basic integrals:

$$I_n = \int \frac{A(t_1, t_2) \bar{F}(t_1) \bar{F}(t_2)}{D_n} d^4 p'', \quad (13)$$

where A is a polynomial, $\bar{F}(t) = F(t)/(t - \lambda^2)$, and

$$\begin{aligned} D_1 &= 1 \\ D_2 &= k''^2 - m^2 \\ D_3 &= p''^2 - M^2 \\ D_4 &= (k''^2 - m^2)(p''^2 - M^2). \end{aligned} \quad (14)$$

Other integrals that can appear are expressed through (13) using symmetry considerations, e.g.

$$\int A(t_1, t_2) \frac{p''^2 - M^2}{k''^2 - m^2} d^4 p'' = \frac{1}{2} \left(1 + \frac{\nu}{4m^2 - t} \right) \int A(t_1, t_2) \frac{t_1 + t_2 - t}{k''^2 - m^2} d^4 p'' - \frac{\nu}{4m^2 - t} \int A(t_1, t_2) d^4 p''. \quad (15)$$

For the x-box diagram the integrals I_1 , I_2 , I_3 , are the same as for the box diagram, but the integral I_4 is not, since the relation between p'' and k'' is different. We denote the corresponding integral I_{4x} .

We will show here in detail the evaluation of the integral I_4 . Other integrals are evaluated similarly. At the end we write down the results for all of them.

As it was discussed previously, the idea is to integrate over two of four integration variables, to obtain

$$I_n = \int \mathcal{K}_n(t_1, t_2) A(t_1, t_2) \bar{F}(t_1) \bar{F}(t_2) dt_1 dt_2 \quad (16)$$

with an explicitly known functions \mathcal{K}_n . This expression can be used for numerical integration or further analysis.

Evaluation of \mathcal{K}_n

We will perform the calculation in the Breit frame. In this frame we have

$$P = \left(\frac{1}{2} \sqrt{4M^2 - t}, 0, 0, 0 \right), \quad q = (0, 0, 0, \sqrt{-t}), \quad K = \left(\frac{\nu}{2\sqrt{4M^2 - t}}, \sqrt{\frac{\nu^2 - (4m^2 - t)(4M^2 - t)}{4(4M^2 - t)}}, 0, 0 \right) \quad (17)$$

(the first is the time component, the following are x -, y -, and z - components). We also denote

$$p'' = (\xi + \frac{1}{2} \sqrt{4M^2 - t}, \rho \cos \phi, \rho \sin \phi, \eta), \quad (18)$$

thus $d^4 p'' = d\xi d\eta \rho d\rho d\phi$. In this notation

$$\begin{aligned} t_{1,2} &= \xi^2 - \rho^2 - (\eta \pm \sqrt{-t}/2)^2, \\ p''^2 - M^2 &= \left(\xi + \frac{1}{2} \sqrt{4M^2 - t} \right)^2 - \eta^2 - \rho^2 - M^2, \\ k''^2 - m^2 &= \left(\frac{\nu}{\sqrt{4m^2 - t}} - \xi \right)^2 - \rho^2 - \eta^2 - m^2 - K_x^2 + 2\rho K_x \cos \phi. \end{aligned} \quad (19)$$

We are to calculate the following integral:

$$I_4 = \int \frac{A(t_1, t_2) \bar{F}(t_1) \bar{F}(t_2)}{(p''^2 - M^2)(k''^2 - m^2)} d\xi d\eta \rho d\rho d\phi. \quad (20)$$

First we integrate over ϕ . The only quantity that does depend on ϕ is k''^2 . Using

$$\frac{1}{2\pi} \int_0^{2\pi} \frac{d\phi}{z - \cos \phi} = \frac{1}{\sqrt{z^2 - 1}} \quad (21)$$

it is easy to verify that

$$\frac{1}{D_\phi} = \frac{1}{2\pi} \int_0^{2\pi} \frac{d\phi}{k''^2 - m^2} = \left[\left(\xi^2 - \frac{\nu}{\sqrt{4M^2 - t}} \xi - \rho^2 - \eta^2 - \frac{t}{4} \right)^2 - 4K_x^2 \rho^2 \right]^{-1/2}. \quad (22)$$

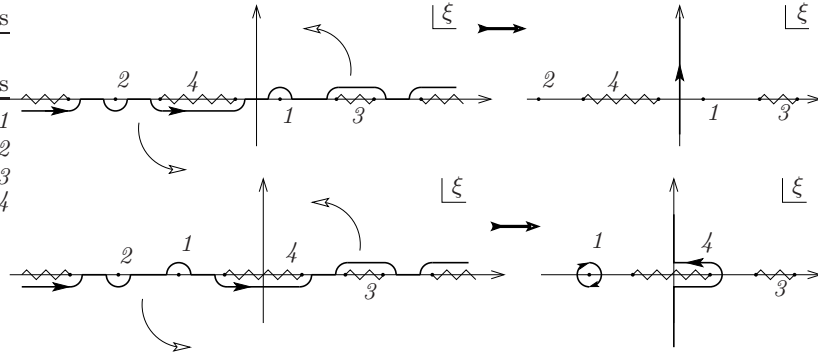


FIG. 3: The integration path before (left) and after Wick rotation (right).

From now on we mean by $\sqrt{z^2 - a^2}$ the analytic function of z with the branch cut from $-a$ to a and $\sqrt{z^2 - a^2} > 0$ for $z > a$. Thus if D_ϕ is real, it has the same sign as the expression in the inner bracket. The integral becomes

$$I_4 = 2\pi \int \frac{A(t_1, t_2) \bar{F}(t_1) \bar{F}(t_2)}{(p''^2 - M^2) D_\phi(\xi, \eta, \rho)} d\xi d\eta \rho d\rho = \int \Phi d\xi d\eta d\rho^2. \quad (23)$$

Next we will integrate over ξ . Here we intend to use Wick rotation, so we need to study the analytic properties of the integrand. The FFs $F(t)$ (and thus $\bar{F}(t)$) are analytic functions of t everywhere in the physical sheet except the positive real axis. Namely, FFs have branch cuts running from $t = (2m_\pi)^2$ to $+\infty$ (m_π is the pion mass) [8], and the additional pole at $t = \lambda^2$ is due to the photon propagator; the physical value is $\bar{F}(t + i0)$. In the complex ξ plane the corresponding singularities lie at $\xi^2 > \rho^2 + (|\eta| - \sqrt{-t}/2)^2$. The factor $1/(p''^2 - M^2)$ has two poles 1 and 2 at $\xi = -\frac{1}{2}\sqrt{4M^2 - t} \pm \sqrt{\rho^2 + \eta^2 + M^2}$ and D_ϕ has two branch cuts 3 and 4 running from $\xi = \frac{\nu}{2\sqrt{4M^2 - t}} \pm \sqrt{(\rho - K_x)^2 + \eta^2 + m^2}$ to $\frac{\nu}{2\sqrt{4M^2 - t}} \pm \sqrt{(\rho + K_x)^2 + \eta^2 + m^2}$. When integrating over ξ , we must pass by these singularities adding $-i0$ to the masses in the usual way. The resulting integration path ℓ is shown in Fig.3 on the left.

Now we perform the Wick rotation to superpose the integration path with the imaginary axis. If the singularities 1 and 3 lie at $\xi > 0$ and 2 and 4 lie at $\xi < 0$, then the integration path can be rotated without crossing them, Fig.3, upper drawing. While singularities 2 and 3 always fulfill the above condition, it may not hold for 1 and 4. In this case an extra terms appear when the path crosses the singularities, Fig.3, lower drawing.

In general case we may write

$$\begin{aligned} \int_\ell \Phi d\xi &= \int_{-i\infty}^{+i\infty} \Phi d\xi + \int \Delta\Phi d\xi \theta(\xi) \theta\left(\frac{\nu}{2\sqrt{4M^2 - t}} - \xi\right) \theta(-D_\phi^2) - \\ &\quad - 2\pi i \int [(p'' - M^2)\Phi] \theta(-\xi) \theta\left(\xi + \frac{1}{2}\sqrt{4M^2 - t}\right) \delta(p''^2 - M^2) d\xi, \end{aligned} \quad (24)$$

where $\Delta\Phi = \Phi(\xi - i0) - \Phi(\xi + i0) = 2\Phi(\xi - i0)$. It can be verified that during the integration according to (24) t_1 and t_2 are always negative. E.g. for the first integral in the r.h.s. $\xi^2 < 0$ and thus $t_{1,2} = \xi^2 - \rho^2 - (\eta \pm \sqrt{-t}/2)^2 < 0$. This is a great advantage, since the FFs are well-known for $t < 0$ (which corresponds to the elastic scattering), and much worse known for $t > 0$.

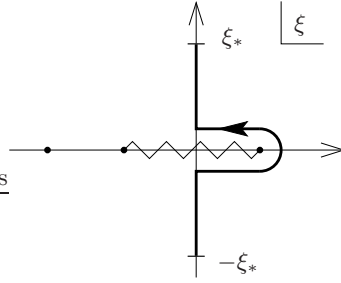
Here we will change variables to make new independent variables (t_1, t_2, ξ) instead of (ρ, η, ξ) . It is important to take into account that $\rho^2 > 0$. This implies the condition: $\xi^2 > \frac{t}{4} - \frac{t_1+t_2}{2} - \frac{(t_1-t_2)^2}{4t}$, and the integration path along the imaginary axis becomes bounded.

It is convenient to introduce the notation

$$\begin{aligned} x_\infty &= \frac{1}{t} \left(\frac{t_1+t_2-t}{2} \right)^2 - \frac{1}{t} t_1 t_2, \\ x_M &= \frac{1}{t} \left(\frac{t_1+t_2-t}{2} \right)^2 - \left(\frac{1}{t} - \frac{1}{4M^2} \right) t_1 t_2, \\ x_m &= \frac{1}{t} \left(\frac{t_1+t_2-t}{2} \right)^2 - \left(\frac{1}{t} - \frac{1}{4m^2} \right) t_1 t_2. \end{aligned} \quad (25)$$

At fixed t_1, t_2 the analytic structure of the integrand differs from described above. It has just one pole and one branch cut (see Fig.4). D_ϕ looks like

$$D_\phi = -\sqrt{4m^2 - t} \sqrt{(\xi - \xi_0)^2 - B^2}, \quad (26)$$

FIG. 4: New integration path ℓ' .

where $\xi_0 = \frac{t_1+t_2-t}{2} \frac{\nu}{(4m^2-t)\sqrt{4M^2-t}}$, $B = \frac{2mK_\nu}{4m^2-t} \sqrt{x_m}$. It is worth noting that (26) may differ in sign from D_ϕ defined according to (22). However along the integration path they are always equal.

After some algebraic transformations we obtain

$$I_4 = \int_{t_1, t_2 \leq 0} \frac{dt_1 dt_2}{2\sqrt{-t}} \left\{ \int_{-i\infty}^{+i\infty} \theta(\xi^2 + x_\infty) \Phi d\xi + \int \Delta \Phi d\xi \theta(\xi) \theta(B^2 - (\xi - \xi_0)^2) - \right. \\ \left. - \frac{2\pi i}{\sqrt{4M^2-t}} \theta(t_1 + t_2 - t) \theta(x_M) \int [(p''^2 - M^2) \Phi] \delta \left(\xi + \frac{t_1+t_2-t}{2\sqrt{4M^2-t}} \right) d\xi \right\}. \quad (27)$$

Now we introduce the integration path ℓ' that passes by the singularities, Fig.4. After that

$$\int_{-i\infty}^{+i\infty} \theta(\xi^2 + x_\infty) \Phi d\xi = \theta(x_\infty) \left\{ \int_{\ell'} \Phi d\xi - \int \Delta \Phi d\xi \theta(\xi) \theta(B^2 - (\xi - \xi_0)^2) - \right. \\ \left. - \frac{2\pi i}{\sqrt{4M^2-t}} \theta(t - t_1 - t_2) \int [(p''^2 - M^2) \Phi] \delta \left(\xi + \frac{t_1+t_2-t}{2\sqrt{4M^2-t}} \right) d\xi \right\} \quad (28)$$

and finally

$$I_4 = \int_{t_1, t_2 \leq 0} \frac{dt_1 dt_2}{2\sqrt{-t}} \left\{ \theta(x_\infty) \int_{\ell'} \Phi d\xi + \theta(x_m) \theta(-x_\infty) \theta(t_1 + t_2 - t) \int \Delta \Phi \theta(B^2 - (\xi - \xi_0)^2) d\xi - \right. \\ \left. - \frac{2\pi i}{\sqrt{4M^2-t}} [\theta(x_\infty) + \theta(x_M) \theta(-x_\infty) \theta(t_1 + t_2 - t)] \int [(p''^2 - M^2) \Phi] \delta \left(\xi + \frac{t_1+t_2-t}{2\sqrt{4M^2-t}} \right) d\xi \right\}. \quad (29)$$

The integration over ξ now can be done analytically. Indeed, according to (23)

$$\Phi = \frac{-\pi}{\sqrt{4m^2-t} \sqrt{4M^2-t}} \frac{A(t_1, t_2) \bar{F}(t_1) \bar{F}(t_2)}{(\xi - \xi_0 - C) \sqrt{(\xi - \xi_0)^2 - B^2}}, \quad (30)$$

where $C = -\frac{t_1+t_2-t}{2\sqrt{4M^2-t}} \left(1 + \frac{\nu}{4m^2-t} \right)$. All factors that depend only on t_1 and t_2 can be factored out. The integration is done using

$$\int \frac{dz}{(z - C) \sqrt{z^2 - B^2}} = \frac{1}{2\sqrt{C^2 - B^2}} \ln \frac{Cz - B^2 - \sqrt{C^2 - B^2} \sqrt{z^2 - B^2}}{Cz - B^2 + \sqrt{C^2 - B^2} \sqrt{z^2 - B^2}}. \quad (31)$$

Here and below $\ln z$ is defined with the branch cut from $z = 0$ to $+\infty$, so that for $z > 0$ $\text{Im} \ln(z + i0) = 0$ and $\text{Im} \ln(z - i0) = 2\pi$. After some simplifications we arrive at the final result of the form (16) with \mathcal{K}_4 which is given below together with other \mathcal{K}_n .

$$\mathcal{K}_1(t_1, t_2) = 2\xi_*\theta(x_\infty), \quad (32)$$

$$\mathcal{K}_2(t_1, t_2) = \frac{1}{\sqrt{4m^2 - t}} \left\{ \theta(x_\infty) \ln \left(\xi + \frac{t_1+t_2-t}{2\sqrt{4m^2-t}} \right) \Big|_{-\xi_*}^{\xi_*} - 2\pi i \theta(x_m)\theta(-x_\infty)\theta(t_1+t_2-t) \right\}, \quad (33)$$

$$\mathcal{K}_3(t_1, t_2) = \frac{1}{\sqrt{4M^2 - t}} \left\{ \theta(x_\infty) \ln \left(\xi + \frac{t_1+t_2-t}{2\sqrt{4M^2-t}} \right) \Big|_{-\xi_*}^{\xi_*} - 2\pi i \theta(x_M)\theta(-x_\infty)\theta(t_1+t_2-t) \right\}, \quad (34)$$

$$\begin{aligned} \mathcal{K}_4(t_1, t_2) = & \frac{1}{\sqrt{R_+}} \left\{ \theta(x_\infty) \ln \left[\xi \sqrt{R_+} - \nu x_\infty + \left(\frac{t_1+t_2-t}{2} \right)^2 \right] \Big|_{-\xi_*}^{\xi_*} + \right. \\ & \left. + 2\pi i \theta(x_\infty) + 2\pi i \theta(-x_\infty)\theta(t_1+t_2-t)[\theta(x_m) + \theta(x_M)] \right\}, \end{aligned} \quad (35)$$

$$\begin{aligned} \mathcal{K}_{4x}(t_1, t_2) = & \frac{-1}{\sqrt{R_-}} \left\{ \theta(x_\infty) \ln \left[\xi \sqrt{R_-} - \nu x_\infty - \left(\frac{t_1+t_2-t}{2} \right)^2 \right] \Big|_{-\xi_*}^{\xi_*} + \right. \\ & \left. + 2\pi i \theta(t_1+t_2-t)[\theta(x_m)\theta(-x_M) + 2\theta(R_-)\theta(x_M)\theta(\nu+t-4M^2)] \right\}, \end{aligned} \quad (36)$$

where $\xi_* = i\sqrt{x_\infty}$ and

$$R_\pm = -\frac{1}{t} \left[\left(\frac{t_1+t_2-t}{2} \right)^2 (\nu \mp t)^2 - t_1 t_2 (\nu^2 - (4m^2 - t)(4M^2 - t)) \right], \quad (37)$$

$\sqrt{R_\pm} = \sigma |R_\pm|^{1/2}$, where $\sigma = -\text{sign}(t_1+t_2-t)$ if $R_\pm > 0$ and $\sigma = -i$ if $R_\pm < 0$.

III. NUMERICAL

It is convenient to distinguish three integration regions: i) $x_\infty \geq 0$ ii) $x_M \geq 0 \geq x_\infty$ and iii) $x_m \geq 0 \geq x_M$. In general case the integrals I_2 , I_4 and I_{4x} contain logarithmic terms like $\ln \frac{m}{\lambda}$ originating from the integration over $x_m \geq 0 \geq x_M$ region. However in actual calculations after adding box and x-box diagrams these logarithms always cancel; it can be shown to be the consequence of gauge invariance. Therefore we may put $m = 0$ if the amplitude is evaluated as a whole (box + x-box).

Before calculating $ep \rightarrow ep$ amplitudes, the following cross-check can be performed. If we omit $A(t_1, t_2)$ and set $F(t) \equiv 1$ in Eq.(13) then the integrals I_n can also be done by usual Feynman parameters method. We have calculated them numerically with different values of M , m , λ , t , ν , and made sure that both methods give identical results.

Now we turn to evaluation of invariant amplitudes \tilde{F}_1 , \tilde{F}_2 , \tilde{F}_3 . Each of them looks like

$$\tilde{F}_i = a_i \ln \lambda + b_i + o(\lambda). \quad (38)$$

The first (IR divergent) term does not contribute to the cross-section if the radiation of soft photons is taken into account. To extract both IR divergent and IR finite part and to simplify the calculation we used the following procedure. We calculated the integrals needed at several small but non-zero λ and fitted obtained values with 3-parameter fit:

$$\tilde{F}_i = a_i \ln \lambda + b_i + c_i \lambda. \quad (39)$$

Though the third term vanishes as $\lambda \rightarrow 0$, it turns out to be necessary to obtain accurate results.

The results obtained by Tsai [2] are

$$\tilde{F}_{1,2}^{(T)} = \frac{\alpha}{\pi} F_{1,2} [K(p, k') - K(p, -k)], \quad \tilde{F}_3^{(T)} = 0, \quad (40)$$

where $K(p_i, p_j) = (p_i \cdot p_j) \int_0^1 \frac{dy}{p_y^2} \ln \frac{p_y^2}{\lambda^2}$, $p_y = p_i y + p_j(1-y)$. In spite of the approximate nature of this result, the terms proportional to $\ln \lambda$ are exact; they are

$$a_{1,2} = a_{1,2}^{(T)} = \frac{2\alpha}{\pi} F_{1,2} \ln \frac{\nu - t}{\nu + t}. \quad (41)$$

Our numerical calculation gave the same results for these terms.

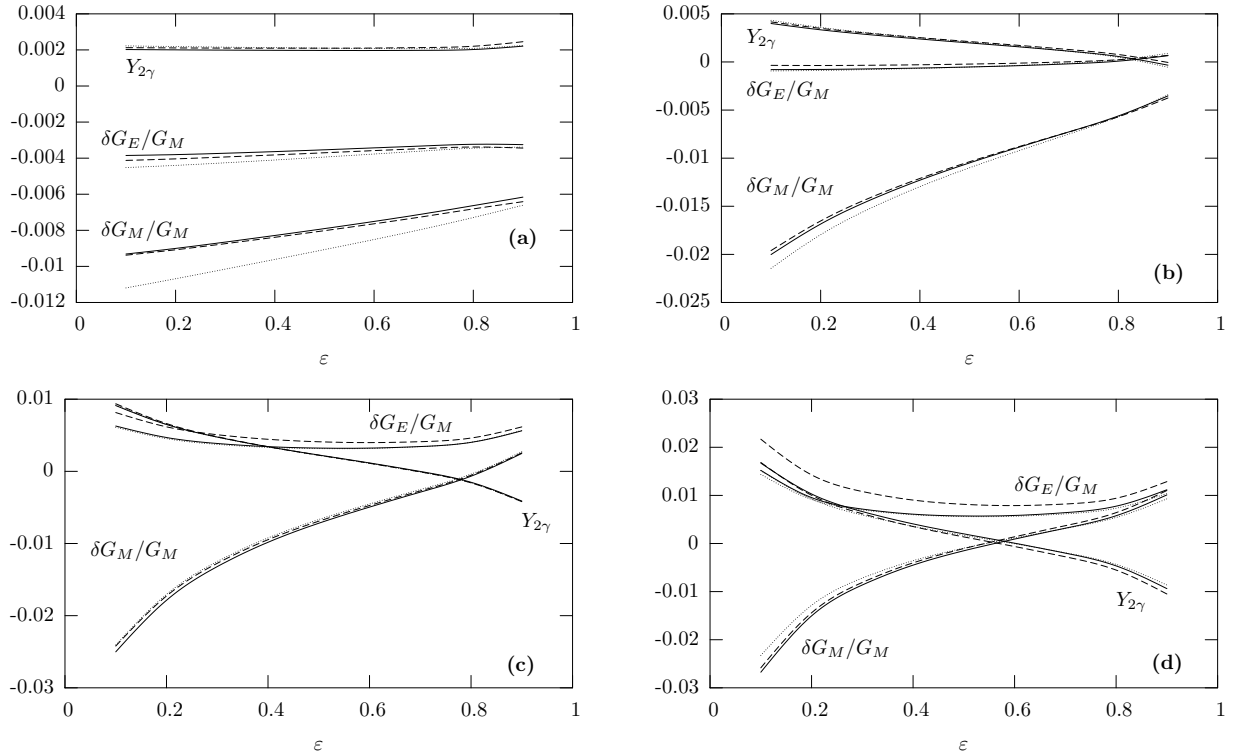


FIG. 5: Two photon exchange corrections $\delta G_M/G_M$, $\delta G_E/G_M$ and $Y_{2\gamma}$ as indicated on the figures, for Q^2 (a) 1 GeV^2 , (b) 3 GeV^2 , (c) 6 GeV^2 , (d) 10 GeV^2 , using form factor parameterization: from Ref.[9] (solid), from Ref.[10] (dashed) and dipole fit (dotted).

Instead of $\tilde{F}_{1,2}$ we introduce linear combinations \tilde{G}_M and \tilde{G}_E exactly as this is done for FFs, $\tilde{G}_E = \tilde{F}_1 - \frac{t}{4M^2}\tilde{F}_2$ and $\tilde{G}_M = \tilde{F}_1 + \tilde{F}_2$. To see the relative size of corrections with respect to the Born approximation, we consider the following quantities:

$$\begin{aligned} \delta G_M/G_M &= (\tilde{G}_M - G_M^{(T)} - G_M)/G_M, \\ \delta G_E/G_M &= (\tilde{G}_E - G_E^{(T)} - G_E)/G_M, \\ Y_{2\gamma} &= (\nu/4M^2)(\tilde{F}_3/G_M). \end{aligned} \quad (42)$$

The results of Tsai are subtracted, since they were used (the therefore already taken into account) in the analysis of almost all experimental data. This is not the same as just drop the logarithmic term, since (40) contains non-logarithmic terms as well.

Note that in contrast to Ref.[6], we normalize δG_E by G_M , rather than G_E . This is done because of great discrepancy in G_E as extracted by two methods; in addition, G_E as extracted by polarization transfer method is close to zero at $Q^2 \approx 6 \text{ GeV}^2$ and $\delta G_E/G_E$ becomes large though δG_E itself is small. On the other hand, the uncertainty in G_M is much smaller.

We have calculated the two photon exchange amplitudes at $Q^2 = 1, 3, 6$ and 10 GeV^2 using three FF parameterizations:

- dipole fit
- fit from Ref.[9] (under assumption $G_E/G_M = \text{const}$)
- fit from Ref.[10] (to data obtained by polarization transfer)

The results are plotted in Fig.5 versus customary parameter ε (virtual photon polarization), $\varepsilon = \frac{\nu^2 + t(4M^2 - t)}{\nu^2 - t(4M^2 - t)}$.

We see that in general results agree with those obtained in Ref.[6]. This is not surprising, because in Sec.II we actually prove that given the FF parameterization which is good for space-like region ($t < 0$) and has correct analytic

properties, the result will not depend on the quality of the fit for $t > 0$ (*a priori* this was not clear). In some sense we justify the approach of Ref.[6]. Nevertheless, our approach is more general, since we can use any FF parameterization.

We also see that the dependence on the choice of FFs is small for $Q^2 < 6 \text{ GeV}^2$, however for the generalized electric FF at $Q^2 = 10 \text{ GeV}^2$ the difference reaches 50% (for small ε).

The absolute value of corrections increases with Q^2 up to $\sim 3\%$ for $\delta G_M/G_M$ at $Q^2 = 10 \text{ GeV}^2$.

The main purpose of this paper is to present new approach for evaluation of two photon exchange diagram. That is why we will not analyze the effect of these corrections on the FF measurements. Such analysis requires evaluation of bremsstrahlung corrections as well, and thus detailed consideration of experimental conditions is needed. We postpone it to another paper.

IV. SUMMARY

We study the two photon exchange in the elastic ep scattering. In this paper we exactly calculate box and crossed-box diagrams with proton in the intermediate state (elastic contribution). Our approach has two main advantages:

- the amplitude is expressed via proton form factors in the space-like region only, Eq.(5). The previous calculations required form factors in the time-like region as well, where they are poorly known.
- any suitable form factor parameterization in the space-like region can be used to evaluate the loop integral. In previous calculations only particular kind of parameterization could be used, since the loop integral was expressed via 4-point functions.

Similar approach can be used to evaluate $\Delta(1232)$ and other resonances contributions, which is currently under investigation.

We have calculated two photon exchange amplitudes using form factors as extracted by Rosenbluth and by polarization transfer methods. The dependence of the result on the choice of form factors is small except the generalized electric form factor for $Q^2 \geq 6 \text{ GeV}^2$.

The same method can be applied to the scattering off any spin-1/2 particle, such as neutron or ${}^3\text{He}$.

[1] M.K. Jones *et al.*, Phys. Rev. Lett. **84**, 1398 (2000); O. Gayou *et al.*, Phys. Rev. Lett. **88**, 092301 (2002); V. Punjabi *et al.*, Phys. Rev. C **71**, 055202 (2005); Erratum-*ibid.*, **71**, 069902 (2005).

[2] Y.S. Tsai, Phys. Rev. **122**, 1898 (1961).

[3] L.C. Maximon, J.A. Tjon, Phys. Rev. C **62**, 054320 (2000).

[4] Yu.M. Bystritskiy, E.A. Kuraev, E. Tomasi-Gustafsson, hep-ph/0603132.

[5] P.G. Blunden, W. Melnitchouk, J.A. Tjon, Phys. Rev. Lett. **91**, 142304 (2003).

[6] P.G. Blunden, W. Melnitchouk, J.A. Tjon, Phys. Rev. C **72**, 034612 (2005).

[7] P.A.M. Guichon, M. Vanderhaeghen, Phys. Rev. Lett. **91**, 142303 (2003).

[8] S. Gasiorowicz, Elementary particle physics (Wiley, New York, 1966).

[9] P.E. Bosted, Phys. Rev. C **51**, 409 (1995).

[10] E.J. Brash, A. Kozlov, S. Li, G.M. Huber, Phys. Rev. C **65**, 051001 (2002).